

Co-Doping Effect of Bismuth Ions on the Gain Characteristics of Er-Doped Silica Optical Fiber

Zexin Zheng, Xiangping Pan , Weizhu Ji, Yanhua Dong , Jianxiang Wen , Wei Chen, Sujuan Huang, Gangding Peng , and Ting-Yun Wang , *Member, IEEE*

Abstract—By examining the spectral and amplification characteristics of Er-doped silica fiber (EDSF) and Bi/Er co-doped silica fiber (BEDSF), an active doped silica fiber with broadband- and flat-gain is investigated. Results show that the bandwidth of BEDSF with a gain greater than 20 dB is approximately 50 nm. Moreover, in the entire C-band, the gain of BEDSF exceeds 26 dB with a fluctuation range of approximately 2 dB. The excellent performance may mainly come from the role of bismuth ions. Further analysis demonstrates that the emission and gain cross-sections are enhanced, the bandwidth is broadened, and the flatness is also optimized by co-doping Bi ions. The fluorescence lifetime of Er³⁺ is lengthened by 1.82 ms, illustrating that there may exist energy transfer from Bi-related active centers to Er³⁺. The results indicate that the proposed BEDSF has significant potential application in optical fiber amplifiers, lasers, sensors, and so on.

Index Terms—Bi/Er co-doped silica fiber, broadband- and flat-gain, gain cross-sections, energy transfer.

I. INTRODUCTION

WITH the advancement of mobile communication systems and internet technologies, a wide variety of innovative applications have emerged, including 6G, cloud data, and machine-to-machine communications. As a result, the demand for optical fiber communication capacity has increased exponentially [1]–[3]. Expanding the transmission bandwidth of fiber amplifiers is an effective approach to meeting these communication demands [4]. Due to the polarization-independent and high output power, Er-doped fiber amplifiers are widely used in optical fiber communication systems. However, the bandwidths of Er ions doped silicate fibers or glasses are limited to a maximum of 40 nm due to the 4f–4f orbital limiting effect [5].

Manuscript received 8 May 2022; revised 2 July 2022; accepted 20 July 2022. Date of publication 26 July 2022; date of current version 17 August 2022. This work was supported by National Key Research and Development Projects under Grant 2020YFB1805800. (*Corresponding author: Ting-Yun Wang.*)

Zexin Zheng, Xiangping Pan, Weizhu Ji, Yanhua Dong, Jianxiang Wen, Wei Chen, Sujuan Huang, and Ting-Yun Wang are with the Key Laboratory of Specialty Fiber Optics and Optical Access Networks, Joint International Research Laboratory of Specialty Fiber Optics and Advanced Communication, Shanghai Institute for Advanced Communication and Data Science, Shanghai University, Shanghai 200444, China (e-mail: zexin159@qq.com; panxiangping@shu.edu.cn; 3186175630@qq.com; dongyanhua@shu.edu.cn; wenjx@shu.edu.cn; 137099465@qq.com; sjhuang@shu.edu.cn; tywang@shu.edu.cn).

Gangding Peng is with the Photonics & Optical Communications, School of Electrical Engineering, University of New South Wales, Sydney 2052, Australia (e-mail: g.peng@unsw.edu.au).

Digital Object Identifier 10.1109/JPHOT.2022.3193901

Hence, finding novel media and studying active doped fibers with ultra-wide bandwidth are vital.

In 2001, Murata et al. discovered that Bi ions exhibited near-infrared fluorescence in SiO₂ glass [6]. Following this discovery, numerous researchers have expressed increasing interest in Bi-doped fibers and glasses. Studies have reported that Bi-doped fibers (BDFs) have broadband gain in the O-, E- or S-band [4], [7], [8]. Some studies have demonstrated that the fluorescence and gain of BDFs in the C- and L-bands are significantly weaker than those in the O-, E- or S-bands [9], [10]. Therefore, BDFs could not be applied in the third optical communication window. Subsequently, Bi/Er co-doped fibers or glasses were developed to achieve ultra-wideband emission. In 2007, Kuwada et al. discovered that Bi-doped SiO₂ glass exhibited ultra-wideband fluorescence in the range of 1100 to 1600 nm by co-doped with Er₂O₃ [11]. In 2011, Peng et al. demonstrated that co-doping Bi ions was an effective method for significantly enhancing the emission intensity near 1.5 μm by suppressing the typical Er-related up-conversion [12]. In 2012, Luo et al. fabricated the first Bi/Er/Al/P co-doped germanium-silicon fiber with ultra-wideband fluorescence covering the O-, E-, S-, C-, and L-bands [13]. In recent years, their team studied the fluorescence mechanism of Bi/Er co-doped fibers (BEDFs) [14], [15] and the effect of post-processing on optical properties [16]–[19], such as heat treatment, quenching, and photo-bleaching. At present, the mechanism by which Bi ions and Er ions interact remains unclear. Additionally, the gain performance and noise figure (NF) of BEDSF have rarely been studied. In 2017, Fistov et al. prepared the Bi/Er co-doped germanosilicate glass to achieve wideband amplification by overlapping emission peaks of the Bi-related active centers (BACs) and Er³⁺. However, the maximum gain is less than 20 dB [20]. In 2018, Zhao et al. reported the maximum on-off gain of the BEDF is only 5.87 dB [15], which leads to difficulties in application in optical communication systems. Therefore, it is imperative to study the effect of doping Bi ions on EDSF and the amplified fiber with high-, broadband-, and flat-gain.

In this study, we used an atomic layer deposition (ALD) method in conjunction with the modified chemical vapor deposition (MCVD) to fabricate an EDSF and a BEDSF. Then we studied the effect of co-doping Bi ions on emission and gain properties of EDSF by analyzing the spectral and amplification performance. In addition, we investigated the absorption, emission and gain cross-sections of two fiber samples. Moreover, the

TABLE I
THE ELEMENT COMPOSITIONS OF TWO FIBER SAMPLES

Element	EDSF (at%)	BEDSF (at%)
Bi	/	0.007
Er	0.026	0.022
P	0.209	0.139
Al	0.251	0.52
Ge	1.711	1.507
O	22.754	23.821
Si	75.049	73.985

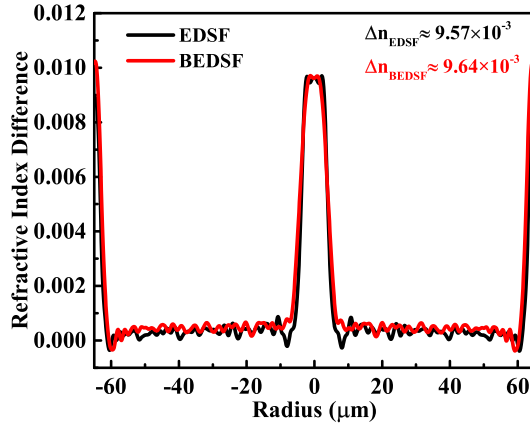


Fig. 1. The refractive index distribution of EDSF and BEDSF.

gain spectra and NF of BEDSF were studied for various pumps and signal powers to optimize gain characteristics and NF.

II. EXPERIMENTAL SECTION

The EDSF and BEDSF were fabricated by ALD (TFS-200, Beneq Inc., Finland) combined with MCVD [21]. Firstly, a SiO₂ porous soot layer was deposited on the inner wall of the silica substrate tube via the MCVD, and then semi-vitrified at a high temperature. Secondly, the Al₂O₃, Bi₂O₃ and Er₂O₃ film were deposited by the ALD process. Here, deionized water was chosen as an oxygen precursor. The Al(CH₃)₃, Bi(thd)₃ (thd = 2, 2, 6, 6-tetramethyl-3, 5-heptanedione) and Er(thd)₃ were the precursors of Al, Bi and Er, respectively. Then, a proper thickness of SiO₂ materials doped with GeO₂ and P₂O₅ was deposited by the MCVD. Finally, the preform was fabricated via collapsing process and then was drawn with a drawing tower. The elemental composition of two fiber samples was determined using an electron probe microanalyzer (Shimadzu EPMA-8050G, Japan). Here, the point scanning was used for analysis. The atomic ratios of Er of two fiber samples are comparable. There are no Bi ions in EDSF, whereas the doping composition of Bi is 0.007 at% in BEDSF. The content of other elements are detailed in Table I. An optical microscope (Olympus BX43, Japan) was used to examine the cross-section. The core diameter of EDSF and BEDSF are 8.09 and 8.64 μm. The refractive index differences of EDSF and BEDSF are approximately 9.57×10^{-3} and 9.64×10^{-3} , respectively, using a digital hologram system [22], as shown in Fig. 1.

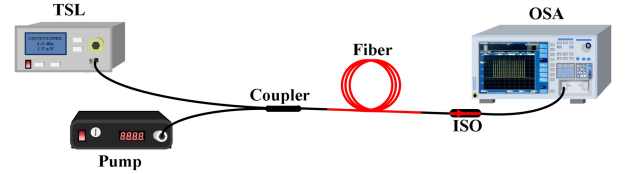


Fig. 2. Experimental schematic of the amplification system with a forward pump.

The absorption spectra of the two fiber samples were determined using the cut-back method with a white light (Yokogawa AQ4305, Japan). The fluorescence and amplified spectra were recorded by an optical spectrum analyzer (OSA, Yokogawa AQ6370D, Japan). The fluorescence decay curves of EDSF and BEDSF were analyzed via a fluorescence spectrometer (FLS 980, Edinburgh Instruments Inc., English). An experimental schematic of the amplification system is depicted in Fig. 2. In this system, the signal was generated using a tunable laser (TSL, Santec TSL-710, Japan) with a linewidth of 100 kHz and a wavelength range of 1480–1640 nm. The pump and the signal light were coupled via a coupler. Isolators were used to protect the lasers and OSA. Typically, the gain is used to describe the amplification characteristics of the fiber. Here, the power of the amplified spontaneous emission (ASE) was determined using the interpolation method. The lengths of fiber samples used in this study are optimal, as follows: EDSF ~ 7 m, BEDSF ~ 8 m.

III. RESULTS AND DISCUSSIONS

A. Absorption and Fluorescence Characteristics

Fig. 3(a) and (b) show the absorption spectra of two fiber samples. The background losses at 1310 nm are approximately 0.06 dB/m in EDSF and 0.064 dB/m in BEDSF, which mainly come from the role of bismuth and erbium ions. The absorption spectra exhibit four strong absorption peaks near 650 nm, 800 nm, 978 nm, and 1535 nm. These absorption peaks correspond to the energy level transitions of the outer electrons of Er³⁺ from the ground state ⁴I_{15/2} to the excited states ⁴F_{9/2}, ⁴I_{9/2}, ⁴I_{11/2}, and ⁴I_{13/2} [23], respectively. The absorption peaks near 980 nm and 1535 nm of the two fiber samples have similar intensities. However, BEDSF has slight blue-shifted absorption peaks and wider bandwidth than that of EDSF, as depicted in the insets of Fig. 3(a) and (b). The full width at half maximum (FWHM) of the absorption peaks of BEDSF near 980 nm and 1535 nm are 24 nm and 40 nm, which are expanded by approximately 4 nm and 12 nm, respectively. The phenomena occur due to the overlap of the absorption peaks of the BACs and Er³⁺. By gaussian multi-peak fitting, the absorption peak at 797 nm of BEDSF is also affected by the absorption of BAC-Si at 812 nm [15]. The absorption peak of BEDSF near 978 nm could be fitted to the absorption peak of Er³⁺ at 976 nm, the peak of BAC-Ge at 950 nm [24], [25], and the peak of BAC-Al at 1000 nm [15]. The absorption peak of BEDSF near 1532 nm also contributes to the absorption peak of BAC-Si at 1420 nm [25]. Furthermore, the intensities of the absorption peaks of BACs (BAC-Ge: ~0.79 dB/m at 950 nm, BAC-Al: ~1.31 dB/m at 1000 nm, BAC-Si: ~0.8 dB/m at

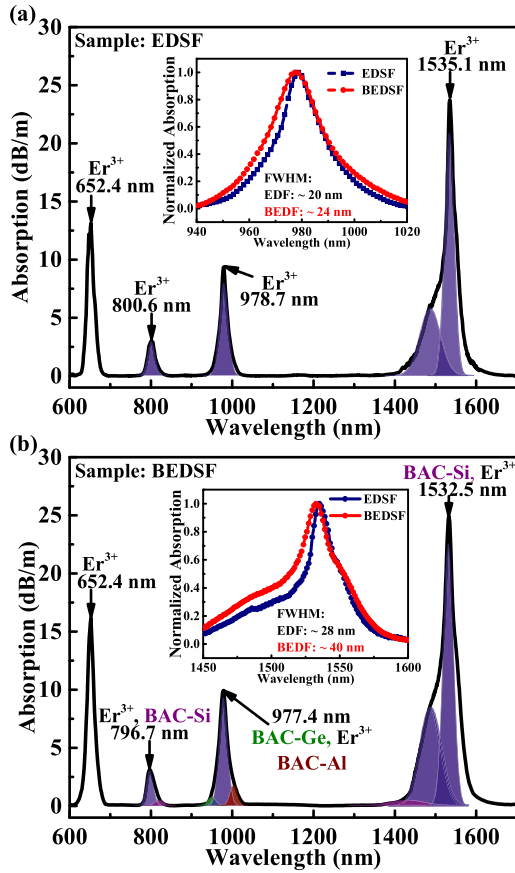


Fig. 3. The absorption spectra of (a) EDSF and (b) BEDSF. The insets are the normalized intensities of the absorption peaks of the two samples: in (a) ~ 980 nm and in (b) ~ 1535 nm.

820 nm and 0.38 dB/m at 1420 nm) are significantly weaker than that of Er^{3+} . This phenomenon could be a result of the decreased Bi-doping concentration.

The absorption cross-sections (σ_a) were then calculated based on the absorption spectra using (1), where N denotes the total number of particles per unit volume and L denotes the length of the sample. The intensities of light before and after passing through the samples are $I_0(\lambda)$ and $I(\lambda)$, respectively.

$$\sigma_a(\lambda) = \frac{1}{NL} \ln \left(\frac{I_0(\lambda)}{I(\lambda)} \right) \quad (1)$$

The maximum absorption cross-sections of BEDSF ($2.55 \times 10^{-25} \text{ m}^2$) near 977 nm is approximately 1.09 times that of EDSF ($2.35 \times 10^{-25} \text{ m}^2$), as shown in Fig. 4(a). The integral absorption cross-section of BEDSF in the range of 910–1050 nm is $6.19 \times 10^{-24} \text{ m}^2$, however, that of EDSF is $4.60 \times 10^{-24} \text{ m}^2$. The absorption cross-section of BEDSF at 1480 nm is $2.12 \times 10^{-25} \text{ m}^2$, which is approximately 1.61 times that of EDSF ($1.32 \times 10^{-25} \text{ m}^2$), as depicted in the inset of Fig. 4(a). Additionally, the integral absorption cross-sections in the range of 1380–1680 nm of two fiber samples are $2.24 \times 10^{-23} \text{ m}^2$ and $3.12 \times 10^{-23} \text{ m}^2$, respectively. These results demonstrate that co-doping Bi ions could increase the pump absorption

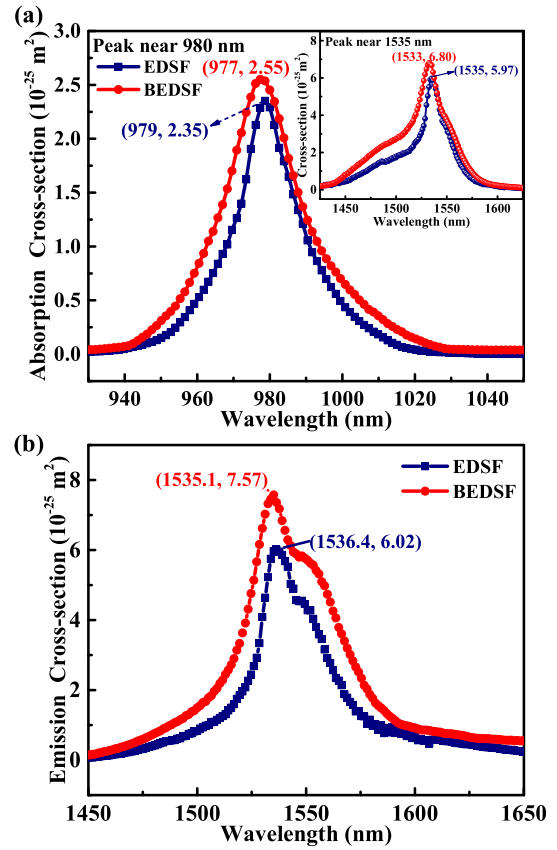


Fig. 4. (a) The absorption cross-sections of the EDSF and BEDSF near 980 nm. The inset shows the absorption cross-sections of the EDSF and BEDSF near 1535 nm. (b) The emission cross-sections of the EDSF and BEDSF.

efficiency and may be beneficial to the enhancement of emission cross-sections.

The emission cross-sections (σ_e) of the two fiber samples were calculated by the McCumber theory [26]. The theory could be described by (2).

$$\sigma_e(\lambda) = \sigma_a(\lambda) \exp \left(\varepsilon - \frac{h\nu}{kT} \right) \quad (2)$$

Where k denotes the Boltzmann constant; T denotes the absolute temperature, and ε is the temperature-dependent excitation energy. The maximum emission cross-section of the BEDSF is approximately 1.26 times that of EDSF, as depicted in Fig. 4(b). And the integral emission cross-section of BEDSF is $3.48 \times 10^{-23} \text{ m}^2$, which is 1.55 times that of EDSF ($2.25 \times 10^{-23} \text{ m}^2$). The results illustrate that the emission cross-section in C- and L-bands is enhanced and widened by co-doping Bi ions, which is conducive to high-, broadband-gain performance and high conversion efficiency.

The forward fluorescence spectra of EDSF and BEDSF with 980 nm and 1480 nm pumps were studied. With a power of 250 mW for the 980 nm pump, the fluorescence intensity of the two fiber samples could reach -12 dBm at 1535 nm. However, when the pump power is 202.8 mW and the pump wavelength is 1480 nm, the fluorescence intensity near 1535 nm is approximately -10 dBm. It is worth noting that the bandwidth of the two

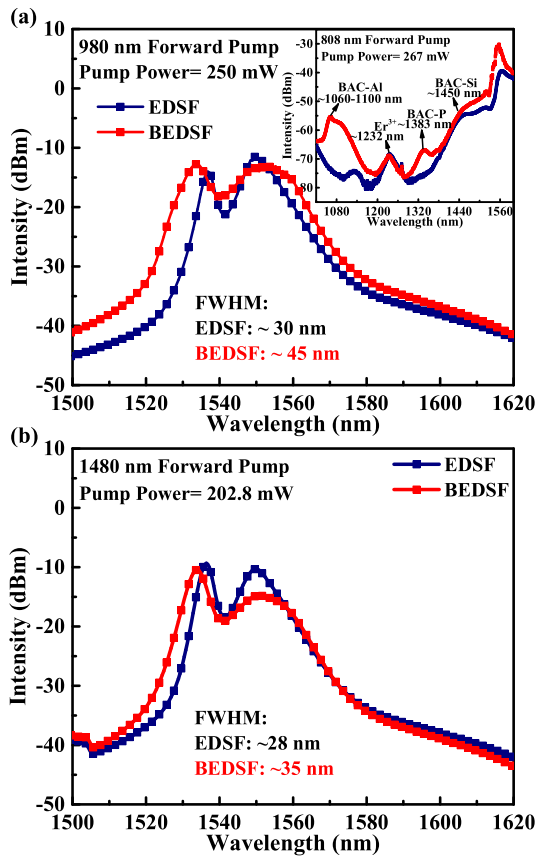


Fig. 5. The forward fluorescence spectra of the EDSF and BEDSF with (a) 980 nm and (b) 1480 nm pumps. The inset in (a) is the forward fluorescence spectra pumped by an 808 nm laser.

fiber samples operated at the 1480 nm pump are narrower than these operated at the 980 nm pump. These phenomena demonstrate that a 1480 nm pump would provide a more efficient conversion [27]. Moreover, the fluorescence intensities of the two fiber samples are comparable, while the BEDSF exhibit a wider fluorescence bandwidth in the range of 1500–1620 nm. BEDSF has an FWHM of 45 nm for pumping at 980 nm, which is approximately 15 nm wider than that of EDSF (~30 nm). These results indicate that co-doping Bi ions would broaden the fluorescence bandwidth and enhance the fluorescence efficiency of Er^{3+} [28]. Additionally, the FWHM of EDSF with a 980 nm pump is comparable to that of a 1480 nm pump, while it of the two pumps differs by 10 nm for BEDSF. In 2019, Zhao et al. [29] reported that the emission centers of Bi-doped fibers varied with the excitation wavelength. Therefore, the observed difference could be due to the significant effect of pump wavelength on BACs. The pump further affects the interaction between BAC and Er ions, thus affecting the fluorescence characteristics.

In general, Bi-doped glasses or fibers exhibit the following fluorescence peaks [30]: BAC-Al (~1100 nm), BAC-P (~1300 nm), BAC-Si (~1420 nm), and BAC-Ge (~1665 nm). The fluorescence peak around 1232 nm is the emission peak of the Er^{3+} , as shown in the inset of Fig. 5(a), which is related to the energy level transition of electrons of Er^{3+} from $^4\text{S}_{3/2}$

to $^4\text{I}_{11/2}$ [31]. And BEDSF exhibits obvious emission peaks of the BACs with an 808 nm pump, as depicted by the red line. The emission peaks correspond to those reported in the literature [14]. The emission peak of BAC-Si could overlap the emission peak of Er^{3+} , which would form broadband emission. However, there has been reported that the maximum FWHM of fluorescence peak of BAC-Si at 1420 nm is 150 nm [25]. And in 2018, Zhao [15] reported that there is no obvious emission peak for BAC-Si with 980 nm pumping. BEDSF also shows no visible emission peaks of BACs under the 980 nm and 1480 nm pumps in our experiments. Therefore, for 980 nm pumping, co-doping Bi ions could not result in a new emission peak that could overlap with the emission peak of Er^{3+} . Co-doping Bi ions may change the local field of Er^{3+} , thus affecting the Stark's split and the fluorescence characteristics of silica fiber. And there may exist energy transfer between BACs and Er^{3+} , affecting the fluorescence efficiency of Er ions.

B. Amplification Characteristics

The BEDSF has a maximum gain of approximately 38.4 dB at 1533 nm when the signal light intensity is -21 dBm and the pump power is 332.4 mW, as shown in Fig. 6(a). And the bandwidth exceeding 20 dB is approximately 50 nm. However, the maximum gain of EDSF at 1550 nm is only 30.5 dB. And the gain exceeds 20 dB only in the range of 1533–1564 nm. The wavelength-dependent gain spectra of the two fibers are depicted in Fig. 6(b) when the signal light intensity is -21 dBm and the 1480 nm pump power is 298.5 mW. The BEDSF has a maximum gain of approximately 35.3 dB at 1535 nm, while the EDSF has a maximum gain of approximately 29.9 dB at 1550 nm. The bandwidth greater than 20 dB of BEDSF (~44 nm) is approximately 12 nm wider than that of EDSF (~32 nm). These results demonstrate that co-doping Bi ions would enhance the gain and broaden the amplification bandwidth. Moreover, for 980 nm pumping, the gain flatness of EDSF and BEDSF are 0.306 and 0.167. The results indicate that the gain flatness of the BEDSF is improved via co-doping Bi ions. It should be noted that the fluorescence intensities of the two fiber samples are comparable, as presented in Fig. 5, however, the gain properties of the BEDSF are superior. The results imply that the BEDSF has a higher conversion efficiency, which may be related to the emission, gain cross-sections and fluorescence lifetime.

The gain spectra and NF of BEDSF were investigated for various pumps and signal powers. The gain is enhanced with the increase of the pump power, while the NF is decreased with the signal power of -21 dBm, as depicted in Fig. 6(c). As the pump power increases, the population of the particles in the stimulated emission process is increased and the intensity of the ASE is also enhanced. However, the rate of gain change with the increase of the pump power is higher than that of ASE. Therefore, the NF is reduced. The gain spectra and NFs of the BEDSF with various signal powers are shown in Fig. 6(d). The inset depicted the variation of the gain and NF with different signal light intensities. As the signal power increases, the gain is decreased and the NF is increased when the pump power is 201 mW. The maximum

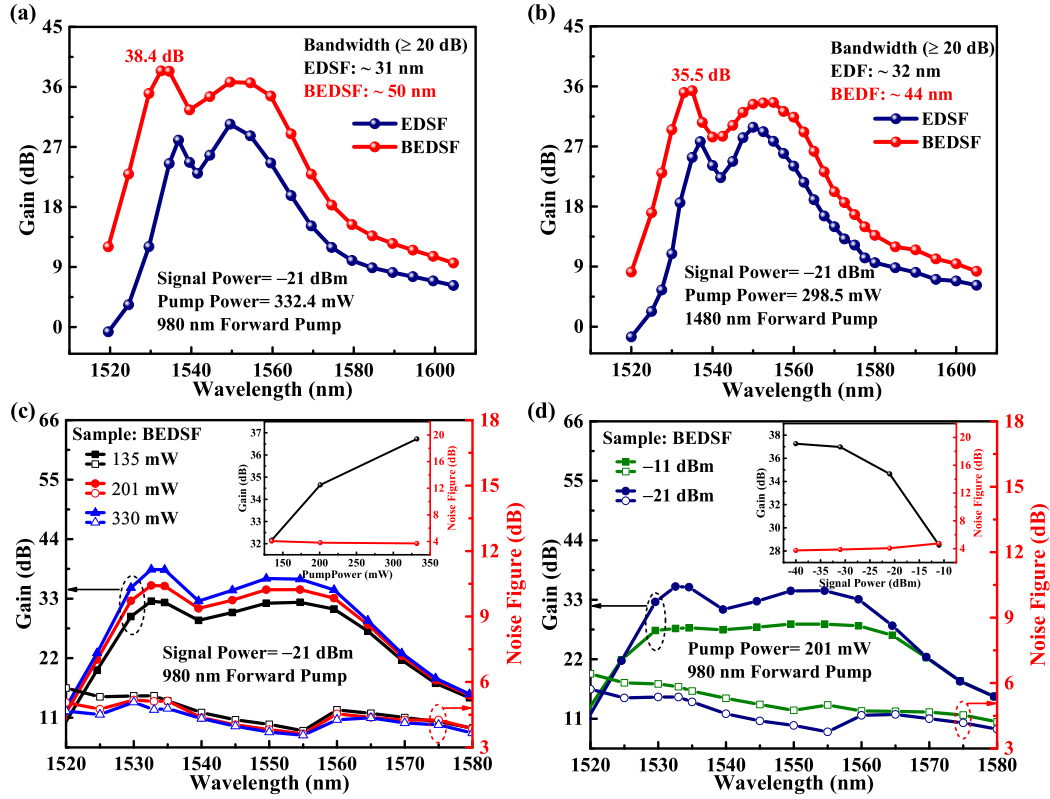


Fig. 6. The gain versus wavelength of EDSF and BEDSF when the signal power is -21 dBm: (a) the pump power is 332.4 mW for the 980 nm pump and (b) the pump power is 298.5 mW for the 1480 nm pump. The gain spectra and NFs of BEDSF at 980 nm pumping with (c) different pump power and (d) different signal power. The insets are the gain and NF of BEDSF at 1550 nm versus pump power (in (c)) and signal power (in (d)).

TABLE II
THE GAIN AND NOISE FIGURE PROPERTIES OF DIFFERENT EDFs AND BEDFS

Samples	Signal power (dBm)	Bandwidths (≥ 25 dB, nm)	Maximum gain (dB)	Gain fluctuation in C-band (dB)	NF in C-band (dB)	Refs. or Expt.
EDF	0	/	22.0	~ 4	/	[32]
ZYAB-EDF	-25	~ 20	25.6	3	<4.2 dB	[34]
HB-EDF ^a	-10	/	~ 11.0	~ 2	<9.0 dB	[33]
BEDF ^b	/	/	13.0	/	/	[35]
BEDF ^b	/	/	5.9	/	/	[15]
BEDSF	-11	~ 40	28.5	2	<5.4 dB	Expt.

^aSingle-stage single-pass.

^bOn-off gain.

gain is up to 41.4 dB at 1533 nm when the signal power is -40 dBm. The NF is approximately 4 dB. Furthermore, when the signal power is -11 dBm, the gain flatness is optimal. The gain is greater than 26 dB over the entire C-band with a fluctuation of approximately 2 dB.

Compare with Er-doped fibers (EDFs) reported and BEDFs reported in literatures [15], [32]–[35], here, BEDSF exhibits excellent amplification characteristics. The gain and noise figure properties of the different fibers, such as the maximum gain, bandwidth greater than 25 dB, gain fluctuation, and NF in the C-band, are listed in detail in Table II. The maximum gain of Er-doped zirconia-yttria-alumina-baria silica fiber (ZYAB-EDF) is comparable to that of BEDSF, while the flatness of ZYAB-EDF is a little worse. And the bandwidth of ZYAB-EDF for the gain

over 25 dB is only 20 nm. The NF of ZYAB-EDF is lower than that of the BEDSF. It is mainly due to the low signal power, -25 dBm. The gain fluctuation in the C-band of the hafnia-bismuth Er co-doped fiber (HB-EDF) and BEDSF are approximately 2 dB, while the maximum gain of HB-EDF is only 11 dB in the single-pass system. In addition, the NF of HB-EDF is higher. The NF of BEDSF is less than 5.4 dB in the entire C-band. Moreover, the maximum on-off gain of the BEDFs is only 13 dB, which limits practical application in optical communication systems. However, the maximum net-gain of BEDSF is up to 41.4 dB. Overall, BEDSF exhibits high-gain characteristics with broad bandwidth and the good flatness.

Furthermore, the product of the FWHM and emission cross-section ($\text{FWHM} \times \sigma_e$) could evaluate the bandwidth properties

TABLE III
THE COMPARISONS OF EMISSION PARAMETERS OF EDSF AND BEDSF

Samples	FWHM (nm)	Maximum σ_e (10^{-25}m^2)	Integral σ_e (10^{-23}m^2)	FWHM $\times\sigma_e$ (10^{-34}m^3)
EDSF	30.4	6.02	2.25	183
BEDSF	45.2	7.57	3.48	342

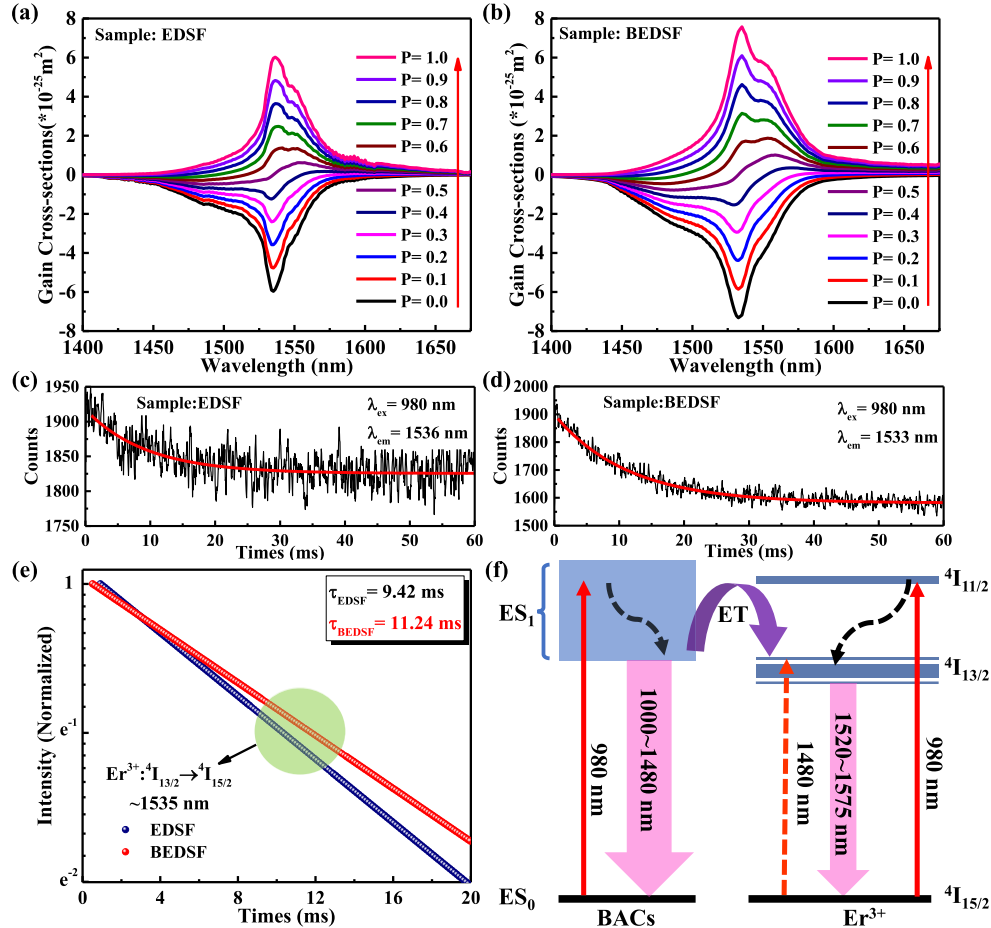


Fig. 7. The gain cross-sections of (a) EDSF and (b) BEDSF. The fluorescence decay curves for 980 nm pumping: (c) EDSF and (d) BEDSF. (e) The normalized intensity of EDSF and BEDSF. (f) The energy transfer diagrams between BACs and Er^{3+} .

of the optical amplifiers [36]. The $\text{FWHM} \times \sigma_e$ of BEDSF is 1.87 times that of EDSF, as detailed in Table III. These results further demonstrate that co-doping with Bi ions would effectively optimize the gain performance.

The gain performance of amplified fiber depends on the emission and gain cross-section (σ_g). The definition of σ_g is given in (3) [37]. Here, P denotes the population inversion, which is the proportion of particles at higher energy levels to the total particles.

$$\sigma_g = P \cdot \sigma_e - (1 - P) \cdot \sigma_a \quad (3)$$

In general, as the pump power increases, the value of P gradually rises and approaches 1.0, corresponding to the gradual rise and saturation of gain. The increase of gain with the pump increasing, as shown in Fig. 6(c), is consistent with the variation

of gain cross-sections. A positive value of the gain cross-section means that the number of particles is reversed, resulting in effective amplification. Fig. 7(a) and (b) show the σ_g of the EDSF and BEDSF, respectively. The maximum gain cross-section of BEDSF ($3.15 \times 10^{-25} \text{m}^2$) is approximately 1.27 times that of EDSF ($2.49 \times 10^{-25} \text{m}^2$) when the population inversion is 0.7. The FWHM of σ_g of BEDSF ($\sim 48 \text{nm}$) is approximately 13 nm wider than that of EDSF ($\sim 35 \text{nm}$). Additionally, the flatness of BEDSF in the range of 1520–1570 nm is approximately 0.163, however, that of EDSF is 0.236. These results further illustrate that co-doping Bi ions would enhance and broaden the gain cross-sections, thus affecting the gain performance and conversion efficiency of the fiber.

As an active center, BACs may have energy transfer with Er ions, which could further affect on the gain characteristics. To study the energy transfer processes, the fluorescence decay

curves at the emission wavelength of 1536 nm for EDSF and 1533 nm for BEDSF were detected with a 980 nm excitation light. The counts were then fitted with a single exponential function, as depicted in red lines in Fig. 7(c) and (d). The decreasing rate of BEDSF intensity was significantly slower than that of EDSF over time, as presented in Fig. 7(e). The fluorescence lifetime of BEDSF is lengthened by 1.84 ms, which indicates that the energy of BACs may be transferred to Er^{3+} and BEDSF has higher conversion efficiency. Based on our observations, we propose the possible energy transfer diagram between Er^{3+} and BACs in the BEDSF pumped by a 980 nm laser, as illustrated in Fig. 7(f). The electrons transition from the ground state to the energy level corresponding to 10241 cm^{-1} by absorbing the energy of the 980 nm laser, as shown by the solid red line. Subsequently, since particles at the high-level are unstable, the electrons at $^4\text{I}_{11/2}$ quickly relax to the lower energy level via non-radiative transitions, after which they emit light at approximately 1530 nm and return to the ground state by the radiative transition. Meanwhile, a portion of the BACs particles at the excited state emit light in the range of 1000–1480 nm and return to the ground state (ES_0). On the one hand, the part fluorescence of BACs would be absorbed by Er^{3+} . On the other hand, the energy of the BACs at the excited state would be directly transferred to Er^{3+} .

IV. CONCLUSION

We investigated a BEDSF with broadband- and flat-gain characteristics by systematically comparing and analyzing the spectral and amplification properties of EDSF and BEDSF. The gain bandwidth of BEDSF greater than 20 dB can reach approximately 50 nm, which is 19 nm wider than that of EDSF. Indeed, the gain fluctuation across the entire C-band is approximately 2 dB and the gain exceeds 26 dB when the signal power is -11 dBm . The BEDSF shows excellent gain characteristics, which may mainly come from the role of bismuth ions. The maximum absorption cross-sections of BEDSF at 980 nm and 1480 nm are 1.09 times and 1.61 times that of EDSF. The results indicate that the pump absorption efficiency of Er ions would be enhanced due to the overlap between the absorption peaks of BACs and Er^{3+} . Moreover, the maximum emission cross-section of the BEDSF is $7.57 \times 10^{-25}\text{ m}^2$, which is approximately 1.26 times that of EDSF. Furthermore, the maximum σ_g of BEDSF is approximately 1.27 times that of EDSF, when the population inversion is 0.7. The FWHM of σ_g of BEDSF is approximately 13 nm wider than that of EDSF. The flatness of BEDSF in the range of 1520–1570 nm is approximately 0.163, while that of EDSF is approximately 0.236. These results illustrate that co-doping Bi ions would enhance and broaden the gain cross-sections, and thus affect the gain performance of the fiber. In addition, the fluorescence lifetime of BEDSF is 11.24 ms, while that of EDSF is only 9.42 ms. Further analysis demonstrates that there may exist the energy transfer from BACs to Er^{3+} , which would enhance the emission intensity and efficiency of Er ions. All the results provide a reference for further optimizing the preparation process and co-doping method to improve the active fiber performance.

REFERENCES

- [1] Y. Yue, J. Zhao, J. Du, and Z. Li, "Special issue on enabling technology in optical fiber communications: From device, system to networking," *Sensors*, vol. 21, no. 6, 2021, Art. no. 1969, doi: [10.3390/s21061969](https://doi.org/10.3390/s21061969).
- [2] J. Hou, "Key technologies on large capacity optical transmission networks," in *Proc. 11th Int. Conf. Power, Energy Elect. Eng., Elect. Netw.*, 2021, pp. 92–98, doi: [10.1109/CPEEE51686.2021.9383329](https://doi.org/10.1109/CPEEE51686.2021.9383329).
- [3] L. Rapp and M. Eiselt, "Optical amplifiers for multi-band optical transmission systems," *J. Lightw. Technol.*, vol. 40, no. 6, pp. 1579–1589, Mar. 2022, doi: [10.1109/jlt.2021.3120944](https://doi.org/10.1109/jlt.2021.3120944).
- [4] A. Donodin et al., "Bismuth doped fibre amplifier operating in E- and S- optical bands," *Opt. Mater. Exp.*, vol. 11, no. 1, pp. 127–135, 2021, doi: [10.1364/OME.411466](https://doi.org/10.1364/OME.411466).
- [5] T. M. Hau et al., "Super broadband near-infrared emission and energy transfer in Bi-Er co-doped lanthanum aluminosilicate glasses," *Opt. Mater.*, vol. 35, no. 3, pp. 487–490, 2013, doi: [10.1016/j.optmat.2012.10.021](https://doi.org/10.1016/j.optmat.2012.10.021).
- [6] Y. Fujimoto and M. Nakatsuka, "Infrared luminescence from bismuth-doped silica glass," *Japanese J. Appl. Phys.*, vol. 40, no. 3B, pp. L279–L281, 2001, doi: [10.1143/JJAP.40.L279](https://doi.org/10.1143/JJAP.40.L279).
- [7] Y. Ososkov et al., "Pump-efficient flattop O+E-bands bismuth-doped fiber amplifier with 116 nm -3 dB gain bandwidth," *Opt. Exp.*, vol. 29, no. 26, pp. 44138–44145, 2021, doi: [10.1364/oe.441775](https://doi.org/10.1364/oe.441775).
- [8] Y. Wang, N. K. Thipparapu, D. J. Richardson, and J. K. Sahu, "Ultra-broadband bismuth-doped fiber amplifier covering a 115-nm bandwidth in the O and E bands," *J. Lightw. Technol.*, vol. 39, no. 3, pp. 795–800, 2021, doi: [10.1109/jlt.2020.3039827](https://doi.org/10.1109/jlt.2020.3039827).
- [9] I. A. Bufetov, S. V. Firstov, V. F. Khopin, O. I. Medvedkov, A. N. Guryanov, and E. M. Dianov, "Bi-doped fiber lasers and amplifiers for a spectral region of 1300–1470 nm," *Opt. Lett.*, vol. 33, no. 19, pp. 2227–2229, 2008, doi: [10.1364/OL.33.002227](https://doi.org/10.1364/OL.33.002227).
- [10] E. M. Dianov, "Amplification in extended transmission bands using bismuth-doped optical fibers," *J. Lightw. Technol.*, vol. 31, no. 4, pp. 681–688, Feb. 2013, doi: [10.1109/JLT.2012.2211569](https://doi.org/10.1109/JLT.2012.2211569).
- [11] Y. Kuwada, Y. Fujimoto, and M. Nakatsuka, "Ultrawideband light emission from bismuth and erbium doped silica," *Japanese J. Appl. Phys.*, vol. 46, no. 4A, pp. 1531–1532, 2007, doi: [10.1143/jjap.46.1531](https://doi.org/10.1143/jjap.46.1531).
- [12] M. Peng, N. Zhang, L. Wondraczek, J. Qiu, Z. Yang, and Q. Zhang, "Ultra-broad NIR luminescence and energy transfer in Bi and Er/Bi co-doped germanate glasses," *Opt. Exp.*, vol. 19, no. 21, pp. 20799–20807, 2011, doi: [10.1364/OE.19.020799](https://doi.org/10.1364/OE.19.020799).
- [13] Y. Luo, J. Wen, J. Zhang, J. Canning, and G. D. Peng, "Bismuth and erbium codoped optical fiber with ultrabroadband luminescence across O-, E-, S-, C-, and L-bands," *Opt. Lett.*, vol. 37, no. 16, pp. 3447–3449, 2012, doi: [10.1364/OL.37.003447](https://doi.org/10.1364/OL.37.003447).
- [14] G. Xiao et al., "Co-doping effect of lead or erbium upon the spectroscopic properties of bismuth doped optical fibres," *J. Lumin.*, vol. 230, 2021, Art. no. 117726, doi: [10.1016/j.jlumin.2020.117726](https://doi.org/10.1016/j.jlumin.2020.117726).
- [15] Q. Zhao, J. Zhang, Y. Luo, J. Wen, and G. D. Peng, "Energy transfer enhanced near-infrared spectral performance in bismuth/erbium codoped aluminosilicate fibers for broadband application," *Opt. Exp.*, vol. 26, no. 14, pp. 17889–17898, Jul. 2018, doi: [10.1364/OE.26.017889](https://doi.org/10.1364/OE.26.017889).
- [16] B. Zhang, S. Wei, M. T. A. Khan, Y. Luo, and G. D. Peng, "Dynamics study of thermal activation of BAC-Si in bismuth/erbium-codoped optical fiber," *Opt. Lett.*, vol. 45, no. 2, pp. 571–574, 2020, doi: [10.1364/ol.384023](https://doi.org/10.1364/ol.384023).
- [17] Q. Zhao, J. Zhang, D. Sporea, Y. Luo, J. Wen, and G. D. Peng, "Gamma radiation and thermal-induced effects on the spectral performance of BACs in Bi/Er codoped aluminosilicate fibers," *Opt. Exp.*, vol. 27, no. 7, pp. 9955–9964, 2019, doi: [10.1364/OE.27.009955](https://doi.org/10.1364/OE.27.009955).
- [18] H. Xu et al., "Effects of quenching and cooling upon near infrared luminescence of Bi/Er co-doped optical fiber," *Opt. Mater. Exp.*, vol. 9, no. 7, pp. 3156–3168, 2019, doi: [10.1364/ome.9.003156](https://doi.org/10.1364/ome.9.003156).
- [19] M. Ding, J. Fang, Y. Luo, W. Wang, and G. D. Peng, "Photo-bleaching mechanism of the BAC-Si in bismuth/erbium co-doped optical fibers," *Opt. Lett.*, vol. 42, no. 24, pp. 5222–5225, 2017, doi: [10.1364/OL.42.005222](https://doi.org/10.1364/OL.42.005222).
- [20] S. V. Firstov et al., "Wideband bismuth- and erbium-codoped optical fiber amplifier for C + L + U-telecommunication band," *Laser Phys. Lett.*, vol. 14, no. 11, 2017, Art. no. 110001, doi: [10.1088/1612-202X/aa8adf](https://doi.org/10.1088/1612-202X/aa8adf).
- [21] J. Wen et al., "Photoluminescence properties of Bi/Al-codoped silica optical fiber based on atomic layer deposition method," *Appl. Surf. Sci.*, vol. 349, pp. 287–291, 2015, doi: [10.1016/j.apsusc.2015.04.138](https://doi.org/10.1016/j.apsusc.2015.04.138).
- [22] C. Yan, S. Huang, Z. Miao, Z. Chang, J. Zeng, and T. Wang, "3D refractive index measurements of special optical fibers," *Opt. Fiber Technol.*, vol. 31, pp. 65–73, 2016, doi: [10.1016/j.yofte.2016.05.007](https://doi.org/10.1016/j.yofte.2016.05.007).

- [23] A. J. Kenyon, "Erbium in silicon," *Semicond. Sci. Technol.*, vol. 20, no. 12, pp. R65–R84, 2005, doi: [10.1088/0268-1242/20/12/r02](https://doi.org/10.1088/0268-1242/20/12/r02).
- [24] B. Yan, Y. Luo, A. Zareanborji, G. Xiao, G. D. Peng, and J. Wen, "Performance comparison of bismuth/erbium co-doped optical fibre by 830 nm and 980 nm pumping," *J. Opt.*, vol. 18, no. 10, 2016, Art. no. 105705, doi: [10.1088/2040-8978/18/10/105705](https://doi.org/10.1088/2040-8978/18/10/105705).
- [25] Y. Luo et al., "Systematical study of up-conversion and near infrared emission of Bi/Er co-doped optical fibre pumped at 830 nm," *Optik*, vol. 133, pp. 132–139, 2017, doi: [10.1016/j.ijleo.2017.01.005](https://doi.org/10.1016/j.ijleo.2017.01.005).
- [26] M. J. F. Digonnet, E. Murphy-Chutorian, and D. G. Falquier, "Fundamental limitations of the McComber relation applied to Er-doped silica and other amorphous-host lasers," *IEEE J. Quantum Electron.*, vol. 38, no. 12, pp. 1629–1637, Dec. 2002, doi: [10.1109/jqe.2002.805111](https://doi.org/10.1109/jqe.2002.805111).
- [27] T. Kashiwada, M. Shigematsu, T. Kougo, H. Kanamori, and M. Nishimur, "Erbium-doped fiber amplifier pumped at 1.48 μm with extremely high efficiency," *IEEE Photon. Technol. Lett.*, vol. 3, no. 8, pp. 721–723, Aug. 1991, doi: [10.1109/68.84464](https://doi.org/10.1109/68.84464).
- [28] Y. Qiu, X. Dong, and C. Zhao, "Spectral characteristics of the erbium-bismuth co-doped silica fibers and its application in single frequency fiber laser," *Laser Phys.*, vol. 20, no. 6, pp. 1418–1424, 2010, doi: [10.1134/s1054660x10110186](https://doi.org/10.1134/s1054660x10110186).
- [29] Q. Zhao, Y. Luo, Y. Dai, and G. D. Peng, "Effect of pump wavelength and temperature on the spectral performance of BAC-Al in bismuth-doped aluminosilicate fibers," *Opt. Lett.*, vol. 44, no. 3, pp. 634–637, 2019, doi: [10.1364/OL.44.000634](https://doi.org/10.1364/OL.44.000634).
- [30] E. G. Firstova et al., "Luminescence properties of IR-emitting bismuth centres in SiO₂-based glasses in the UV to near-IR spectral region," *Quantum Electron.*, vol. 45, no. 1, pp. 59–65, 2015, doi: [10.1070/QE2015v045n01ABEH015624](https://doi.org/10.1070/QE2015v045n01ABEH015624).
- [31] B. Zhou, L. Tao, Y. H. Tsang, W. Jin, and E. Y. B. Pun, "Superbroadband near-infrared emission and energy transfer in Pr³⁺-Er³⁺ codoped fluorotellurite glasses," *Opt. Exp.*, vol. 20, no. 11, pp. 12205–12211, 2012, doi: [10.1364/OE.20.012205](https://doi.org/10.1364/OE.20.012205).
- [32] R. Dardaillon et al., "Broadband radiation-resistant erbium-doped optical fibers for space applications," *IEEE Trans. Nucl. Sci.*, vol. 64, no. 6, pp. 1540–1548, Jun. 2017, doi: [10.1109/tns.2017.2701550](https://doi.org/10.1109/tns.2017.2701550).
- [33] A. A. Al-Azzawi et al., "An efficient wideband hafnia-bismuth erbium co-doped fiber amplifier with flat-gain over 80 nm wavelength span," *Opt. Fiber Technol.*, vol. 48, pp. 186–193, 2019, doi: [10.1016/j.yofte.2019.01.012](https://doi.org/10.1016/j.yofte.2019.01.012).
- [34] J. Duarte et al., "Optical amplification performance of erbium doped zirconia-yttria-alumina-baria silica fiber," *Opt. Mater. Exp.*, vol. 9, no. 6, pp. 2652–2661, 2019, doi: [10.1364/ome.9.002652](https://doi.org/10.1364/ome.9.002652).
- [35] W. Liu et al., "Spectral characteristics of Bi/Er co-doped silica fiber fabricated by atomic layer deposition (ALD)," in *Proc. Asia Commun. Photon. Conf.*, 2015, pp. 1–3.
- [36] J. Yang et al., "Effect of Bi₂O₃ on the spectroscopic properties of erbium-doped bismuth silicate glasses," *J. Opt. Soc. Amer. B*, vol. 20, no. 5, pp. 810–815, 2003, doi: [10.1364/JOSAB.20.000810](https://doi.org/10.1364/JOSAB.20.000810).
- [37] J. Mendez-Ramos, V. K. Tikhomirov, A. B. Seddon, and V. D. Rodriguez, "Flat gain cross-section of 1.5 μm amplifier in Er³⁺-doped oxyfluoride glass-ceramics," *Physica Status Solidi (a)*, vol. 201, no. 9, pp. R57–R59, Jul. 2004, doi: [10.1002/pssa.200409046](https://doi.org/10.1002/pssa.200409046).